Multiband Antenna Q Optimization using Stored Energy Expressions

Cismasu, Marius; Gustafsson, Mats

2014

CODEN:LUTEDX/(TEAT-7230)/1-9/(2014)

Multiband Antenna Q Optimization using Stored Energy Expressions

Marius Cismasu and Mats Gustafsson

Electromagnetic Theory
Department of Electrical and Information Technology
Lund University
Sweden

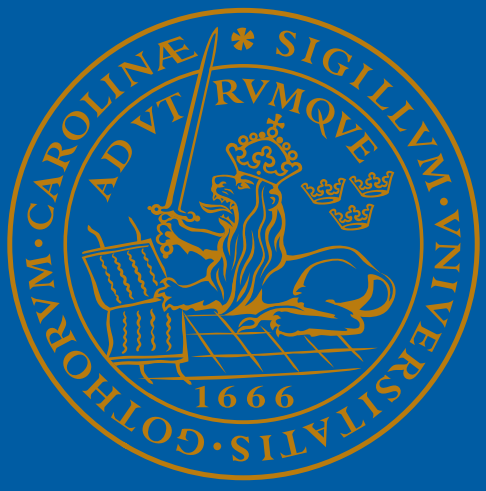

(TEAT-7230)/1-9/(2014): M. Cismasu & M. Gustafsson, Multiband antenna Q optimization using stored energy expressions

Marius Cismasu and Mats Gustafsson
{Marius.Cismasu, Mats.Gustafsson}@eit.lth.se

Department of Electrical and Information Technology
Electromagnetic Theory
Lund University
P.O. Box 118
SE-221 00 Lund
Sweden

Editor: Gerhard Kristensson

Abstract

A method to compute antenna Q from a single frequency current distribution is applied to the optimization of multiband radiating structures. A genetic algorithm produces suboptimal structures in the sense of simultaneous multiband minimum Q. These structures model in a simplified manner common wireless communication devices. The comparison with the physical bounds for the considered situations shows that the suboptimal structures perform close to their limitations. Matching networks are designed using real component models with a commercial tool. These networks have less than three components and provide less than -6.5 dB reflection coefficient magnitude in all considered bands. The results show that the single frequency Q estimation method may be useful for antenna design.

1 Introduction

A method to compute antenna Q from a single frequency current excited on a radiating structure is presented in [7, 9], see also [10]. This method is based on stored electric and magnetic energy [5, 18] and radiated power expressions in terms of the current. The Q estimation method is applied in a genetic algorithm and method of moments (GA/MoM) [13, 16] scheme to optimize antenna Q and resonance at single frequencies in [3].

Here we apply the above introduced method to the multiband Q optimization of rectangular radiating structures with rectangular ground planes. Such structures model in a simplified manner common wireless communication terminals. An improved version of the genetic algorithm produces structures which are less prone to unpredictable behavior due to genetic characteristics such as isolated single mesh element metallic patches. The optimized structure input impedance is computed using the commercial electromagnetic solver ESI-CEM [4]. This result is used in the software tool BetaMatch [2] to design a matching network for all considered bands. The results show that the Q estimation method from the energy stored in excited fields and radiated power may be useful for the design process of radiating structures.

The comparison with the physical bounds for structures with a rectangular ground plane [7] shows that the optimized structures perform close to their physical limitations. Such a comparison can be used to stop an optimization process or assess the realizability of design specifications.

The paper is organized as follows. The results of the theory presented in [3, 7, 9] are included in Sec. 2. The multiband antenna objective function for optimization is introduced in Sec. 3. The setup used for obtaining the results of Sec. 4 is described in Sec. 4.1. Structures optimized using the GA/MoM scheme and their performance are presented in Sec. 4.2. The paper ends with conclusions, Sec. 5.

2 Antenna Q and Stored Energies

The quality factor of a lossless, resonant or nonresonant, antenna is defined as [19]

$$Q = \frac{2\mathrm{c}_0 k \max\{W_\mathrm{e}, W_\mathrm{m}\}}{P_\mathrm{rad}}, \tag{2.1}$$

where c_0 is the speed of light in free space, k is the wavenumber, W_e and W_m are respectively the electric and magnetic energies stored in the fields excited by the antenna, and P_r is the power radiated by the antenna. This definition is equivalent to that in [1] for resonant antennas.

We consider infinitely thin lossless perfectly electrically conducting (PEC) structures in vacuum on which surface current densities $\boldsymbol{J}$ may be excited. Such currents are approximated using a set of basis functions $\boldsymbol{\psi}_p$ as

$$\boldsymbol{J}(\boldsymbol{r}) \approx \sum_{p=1}^{N} J_p \boldsymbol{\psi}_p(\boldsymbol{r}), \tag{2.2}$$

where $\boldsymbol{r}$ is the position vector and $\mathbf{J} = (J_1, J_2, \ldots, J_N)^\mathrm{T}$ is a matrix of complex expansion coefficients. These coefficients are used to approximate the stored electric and magnetic energies and radiated power in (2.1) as

$$W_\mathrm{e} \approx \frac{\mu_0}{4k} \sum_{p=1}^{N} \sum_{q=1}^{N} J_p^* X_{\mathrm{e},pq} J_q = \frac{\mu_0}{4k} \mathbf{J}^\mathrm{H} \mathbf{X}_\mathrm{e} \mathbf{J}, \tag{2.3}$$

$$W_\mathrm{m} \approx \frac{\mu_0}{4k} \sum_{p=1}^{N} \sum_{q=1}^{N} J_p^* X_{\mathrm{m},pq} J_q = \frac{\mu_0}{4k} \mathbf{J}^\mathrm{H} \mathbf{X}_\mathrm{m} \mathbf{J}, \tag{2.4}$$

and

$$P_\mathrm{r} \approx \frac{\eta_0}{2} \sum_{p=1}^{N} \sum_{q=1}^{N} J_p^* R_{\mathrm{r},pq} J_q = \frac{\eta_0}{2} \mathbf{J}^\mathrm{H} \mathbf{R}_\mathrm{r} \mathbf{J}, \tag{2.5}$$

where μ_0 and η_0 are the free space permeability and impedance respectively, $\mathbf{X}_\mathrm{e}$ and $\mathbf{X}_\mathrm{m}$ are the electric and magnetic reactance matrices, and $\mathbf{R}_\mathrm{r}$ is the radiation resistance matrix. These matrices have been introduced in [7, 9], see also [10]. Quadratic forms similar to those in (2.5) have been employed for antenna array optimization in free space [11]. Replacing (2.3), (2.4) and (2.5) in (2.1) we obtain:

$$Q \approx \frac{\max\{\mathbf{J}^\mathrm{H} \mathbf{X}_\mathrm{e} \mathbf{J}, \mathbf{J}^\mathrm{H} \mathbf{X}_\mathrm{m} \mathbf{J}\}}{\mathbf{J}^\mathrm{H} \mathbf{R}_\mathrm{r} \mathbf{J}}. \tag{2.6}$$

The expansion coefficients in (2.2) can be computed using an electromagnetic solver, *e.g.*, ESI-CEM [4] or any other commercial solver. An EFIE (Electric Field Integral Equation) based MoM (Method of Moments) solver is straightforwardly customizable for the computation of the matrices $\mathbf{X}_\mathrm{e}$, $\mathbf{X}_\mathrm{m}$ and $\mathbf{R}_\mathrm{r}$, [3, 7, 9]. This customization does not add a significant computational overhead to the original EFIE impedance matrix, $\mathbf{Z}$, computation [11, 12, 15]. Furthermore the previously mentioned four matrices are readily suitable for GA/MoM [13] optimization.

3 Multiband Antennas

Many hand-held mobile terminals support communication standards that operate in different frequency bands. One solution to accommodate this multiband requirement is to use antennas that perform acceptably well in all frequency bands needed for communication. In addition to multiband antennas matching networks are usually used to connect antennas to transceiver chains. These matching networks improve the intrinsic power transfer capability between transceiver and antenna and mitigate some effects of the changing communication environment on antenna performance.

We optimize the structures for minimum Q at the center frequency of each band of interest. The optimized structures are then simulated using the commercial solver ESI-CEM [4]. The input impedance obtained from the commercial solver is used in BetaMatch [2] to optimize a matching network for multiband operation. The results show that the stored energies (2.3) and (2.4) may be useful for automating part of the design process of mobile terminal antennas.

The GA/MoM procedure [13, 16, 17] is used to obtain suboptimal structures in the sense of multiband operation. An in-house genetic algorithm [3] searches the rows and columns of an impedance matrix that minimize the objective function

$$F_{\mathrm{C}} = \alpha_{\mathrm{M}} \max \left\{ \frac{Q_b}{Q_{\mathrm{T},b}} \right\}_{b=1,2,\ldots,N_{\mathrm{b}}} + \alpha_{\mathrm{S}} \sum_{b=1}^{N_{\mathrm{b}}} \frac{Q_b}{Q_{\mathrm{T},b}}, \tag{3.1}$$

where Q_b is the quality factor (2.6) at the center frequency of band b, $Q_{\mathrm{T},b}$ is the quality factor required for the antenna to meet the specifications in band b, N_{b} is the total number of frequency bands where the structure should operate, and α_{M} and α_{S} are weights associated with the maximum and sum of the normalized Q factors for each band. Equation (3.1) is an example as different optimization criteria lead to different objective functions.

4 Results

4.1 Simulation Setup

Mobile terminals may be modeled, in a simplified manner, as rectangular regions. We consider, for further simplification, infinitely thin PEC radiating structures limited to a rectangular region with the length $\ell = 13\mathrm{cm}$ and width $w = 6.5\mathrm{cm}$. A small, rectangular part of this region, the "antenna region", is dedicated to a structure fed by the transmitter(s), see Fig. 1. The structure in the antenna region is not necessarily rectangular. Here this structure is obtained through a process of GA/MoM optimization [13]. The remaining rectangular, usually larger, part of the region is considered entirely metallic and fixed. This part acts as a ground plane for the structure in the antenna region, contributing to the radiation of the structure. We refer to this part as the "ground plane" in the following.

The "mother" structure [13, 16] for the simplified situation above is a metallic, rectangular region of the same dimensions ℓ and w. This structure represents the

maximum extent PEC metal may have in the radiating device. The mother structure is divided into $N_x = 120$ by $N_y = 60$ rectangular mesh elements in the $\hat{\boldsymbol{x}}$ and $\hat{\boldsymbol{y}}$ directions, respectively. Note that in this particular case the mesh elements are square. This discretization is used both in the MoM impedance matrix computation and in the genetic optimization.

An in-house EFIE based electromagnetic solver is used to compute the matrices $\mathbf{Z}$, $\mathbf{X}_{\rm e}$, $\mathbf{X}_{\rm m}$ and $\mathbf{R}_{\rm r}$ for the mother structure. This solver uses Galerkin testing [15] with rooftop basis and testing functions. These functions are defined on pairs of adjacent mesh elements, *i.e.*, elements sharing a common edge, [14]. Their amplitudes are linearly increasing towards the common edge. Their directions are perpendicular to the common edge, pointing from the first to the second mesh element (considering a fixed mesh element numbering rule). The four matrices mentioned above are square with $N = 2N_xN_y - N_x - N_y = 14220$ rows.

Three frequency bands have been chosen to illustrate the Q computation procedure. These bands are 699 – 746, 880 – 960 and 1710 – 1990 MHz. The electrical sizes of the structure for the center frequencies are $k\ell \approx 1.97$, 2.5, and 5.04. The mother matrices $\mathbf{Z}_b$, $\mathbf{X}_{{\rm e},b}$, $\mathbf{X}_{{\rm m},b}$ and $\mathbf{R}_{{\rm r},b}$ are computed using the in-house solver described above for the center frequency of each band, indexed by $b = 1$, 2, 3.

A block matrix decomposition [13] is performed on each of the twelve mother matrices introduced in the previous paragraph. Denote $\mathbf{X} \in \{\mathbf{Z}_b, \mathbf{X}_{{\rm e},b}, \mathbf{X}_{{\rm m},b}, \mathbf{R}_{{\rm r},b}\}_{b=1,\,2,\,3}$ one of these mother matrices. Each element of this matrix corresponds to a pair of basis and test functions. Considering a borderline between a metallic ground plane and an antenna region (*e.g.*, the line along which F is located in Fig. 1) we write

$$\mathbf{X} = \begin{pmatrix} \mathbf{X}_{\rm AA} & \mathbf{X}_{\rm AG} \\ \mathbf{X}_{\rm GA} & \mathbf{X}_{\rm GG} \end{pmatrix}.$$

The elements of $\mathbf{X}$ with the corresponding basis and test functions entirely in the antenna region or across the borderline are grouped into the first block, $\mathbf{X}_{\rm AA}$. The elements with basis and test functions entirely in the ground plane are grouped into the block $\mathbf{X}_{\rm GG}$. The last two blocks have basis functions in the antenna region/across the border (ground plane) and test functions in the ground plane (antenna region/across the border), $\mathbf{X}_{\rm AG}$ ($\mathbf{X}_{\rm GA}$). The natural overlapping of the rooftop function domains of definition allows the existence of closed loops of metal ground–antenna region–ground.

The sizes of the matrices manipulated during optimization reduce using block matrix decomposition. The EFIE MoM system of equations is written for each frequency

$$\begin{pmatrix} \mathbf{Z}_{\rm AA} & \mathbf{Z}_{\rm AG} \\ \mathbf{Z}_{\rm GA} & \mathbf{Z}_{\rm GG} \end{pmatrix} \begin{pmatrix} \mathbf{J}_{\rm A} \\ \mathbf{J}_{\rm G} \end{pmatrix} = \begin{pmatrix} \mathbf{V} \\ \mathbf{0} \end{pmatrix}, \tag{4.1}$$

where $\mathbf{J}_{\rm A}$ and $\mathbf{J}_{\rm G}$ are the blocks of basis function coefficients that define the current flowing on the antenna region and ground plane respectively, $\mathbf{V}$ is a matrix that models the feeding of the structure, *e.g.*, a voltage gap, and the frequency band index has been omitted. Considering the structure fed only in the antenna region

the current is

$$\left\{ \begin{array}{rcl} \mathbf{J}_{\mathrm{A}} & = & (\mathbf{Z}_{\mathrm{AA}} - \mathbf{Z}_{\mathrm{AG}}\mathbf{Z}_{\mathrm{GG}}^{-1}\mathbf{Z}_{\mathrm{GA}})^{-1}\mathbf{V} \\ \mathbf{J}_{\mathrm{G}} & = & -\mathbf{Z}_{\mathrm{GG}}^{-1}\mathbf{Z}_{\mathrm{GA}}\mathbf{J}_{\mathrm{A}} = \mathbf{T}\mathbf{J}_{\mathrm{A}} \end{array} \right. \tag{4.2}$$

The quadratic forms in (2.3), (2.4) and (2.5) take the form

$$\mathbf{J}^{\mathrm{H}}\mathbf{X}\mathbf{J} = \mathbf{J}_{\mathrm{A}}^{\mathrm{H}} \left(\mathbf{X}_{\mathrm{AA}} + 2\,\mathrm{Re}\{\mathbf{X}_{\mathrm{AG}}\mathbf{T}\} + \mathbf{T}^{\mathrm{H}}\mathbf{X}_{\mathrm{GG}}\mathbf{T} \right) \mathbf{J}_{\mathrm{A}}, \tag{4.3}$$

where $\mathbf{X} \in \{\mathbf{X}_{\mathrm{e}}, \mathbf{X}_{\mathrm{m}}, \mathbf{R}_{\mathrm{r}}\}$. The block matrix decomposition is applied to the original mother matrices prior to the optimization procedure. The optimization algorithm searches the rows and columns of the matrices in parentheses in (4.2) and (4.3) that minimize the objective function (3.1). These latter matrices may be considered "mother" matrices for the optimization process. Their size is given by the size and shape of the antenna region. For example, in the case of a rectangular antenna region occupying 20% of the entire structure area as in Fig. 1, the size of the matrices in parentheses is 2856×2856.

An in-house genetic algorithm [3] is used to optimize the structures. This algorithm uses a population of 200 individuals out of which 80 are randomly chosen for tournament selection. The two point crossover probability is 0.8. A maximum of six genes at once are mutated with a probability of 20% if improvement of the objective function occurs within 100 iterations. After 100 iterations without improvement up to ten genes at once are mutated with 100% probability. The algorithm stops if the objective function does not improve during 50 generations, *i.e.*, 10^4 iterations.

The genetic algorithm is neither an exhaustive search of the optimum solution nor an exhaustive evaluation of the characteristics of a suboptimal solution. This algorithm uses genetic principles to drive an initially random population towards a suboptimal solution avoiding to some extent local extrema. Genetic principles allow the appearance of unwanted characteristics of offspring ("malformations"). For instance there may appear isolated single mesh element metallic patches or double 90° metallic bends diagonally interconnected (*i.e.*, corner connections). Such characteristics might have unpredictable effects on the manufactured structure performance. This is why such traits are specially "purged" after each offspring generation.

The objective function (3.1) minimized by the GA is

$$F_{\mathrm{C}} = \max\left\{ \frac{Q_1}{16}, \frac{Q_2}{12}, \frac{Q_3}{7} \right\} + 0.1 \left(\frac{Q_1}{16} + \frac{Q_2}{12} + \frac{Q_3}{7} \right). \tag{4.4}$$

The values 16, 12 and 7 are computed for less than -6 dB reflection coefficient magnitude at the antenna input in all frequency bands [19].

The solutions obtained through optimization are simulated using the commercial solver ESI-CEM [4]. The input impedance computed by this solver is used in BetaMatch [2] to design a matching network. Models of large SMD (surface-mount devices) have been employed for matching. However not all optimized structures could be matched in all bands with realistic component models. In these situations matching with ideal components has been attempted.

The Q factors of the optimized structures are compared with the physical bounds [7, 9] for rectangular structures with a fixed rectangular ground plane. Here we

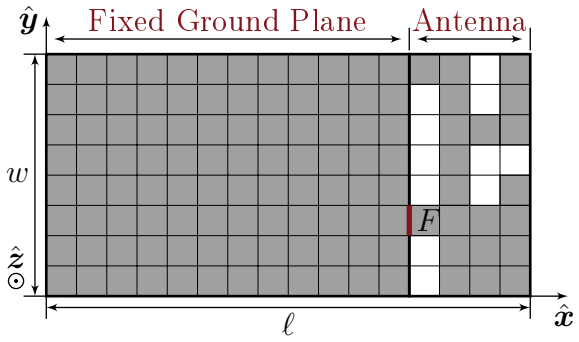

Figure 1: Example of discretized radiating structure with a fixed rectangular ground plane. Gray shaded elements represent metallic patches. The feeding edge is marked with F.

maximize the $\hat{\boldsymbol{z}}$ directivity – antenna Q (D/Q) quotient to derive the physical bound for the Q factor. For illustration purpose the Q factors are also compared with the physical bound [6, 8] for structures limited to rectangular regions. This latter bound is derived assuming the structures electrically small, $ka \ll 1$, radiating as an electric dipole with directivity approximately 1.5. Such comparisons with physical bounds may be used as stopping criteria for optimization algorithms applied to electrically small structures. For electrically large structures the physical bounds on Q [6–9] are less useful as the Q is very small and the antennas do not radiate mainly in the $\hat{\boldsymbol{z}}$ direction.

4.2 Simple Phone Model

The structures optimized for multiband operation are exemplified in Fig. 1. Three sizes of the antenna region have been imposed: 20, 15 and 10% of the entire structure area at one end in the ℓ direction. The feed has been placed at three fixed positions, all on the borderline between the ground plane and antenna region. These positions are the side, middle, and half way between side and middle in the w direction, *i.e.*, $y \approx 0.54$, 16.8, and 32mm, respectively. The optimization algorithm has been run five times for each of the nine resulting combinations of antenna region size and feed position. The optimized antenna regions of the structures with the smallest objective function (4.4) per combination of antenna region size and feed position are depicted in Fig. 2.

The Q factors (2.6) of the optimized structures depicted in Fig. 2 middle column are compared with the physical bounds [6–9] in Fig. 3 for electrical dimensions commonly accepted as small. These structures have the smallest objective function (3.1) compared with structures with the same size but different feeding positions. Simple matching networks are designed for the structures in Fig. 2 middle column using real component models in BetaMatch [2]. These networks, depicted in Fig. 4, allow matching to less than -6.5dB reflection coefficient magnitude throughout all frequency bands.

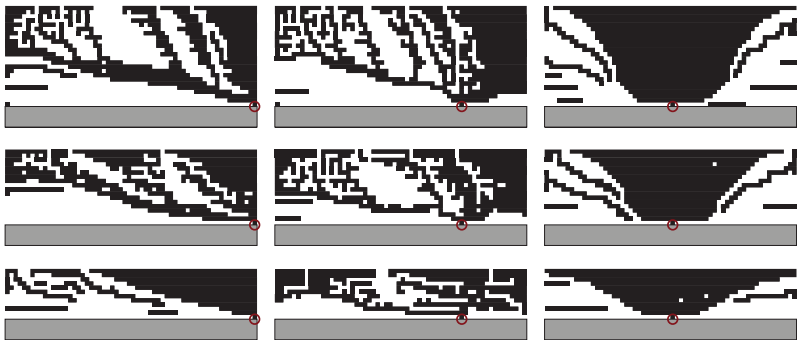

Figure 2: Example of antenna regions of structures optimized for multiband minimum Q. Rectangular regions $130 \times 65\,\mathrm{mm}^2$ with fixed rectangular ground planes and antenna regions extending 20% (top row), 15% (middle row), and 10% (bottom row) of the entire structure area as depicted in Fig. 1. Fixed feeding edges are circled. Part of the ground plane is shaded.

5 Conclusions

A method of computing antenna Q from a single frequency current distribution [7, 9, 18] is used in a GA/MoM [13] scheme to optimize rectangular radiating structures for simultaneous multiple band minimum Q. A significant part of these structures is a fixed metallic ground plane such that these structures model in a simplified manner common wireless communication devices. The optimized antenna Q factors have been compared with the physical bounds corresponding to the analyzed situations. This comparison shows that the suboptimal solutions perform close to the physical bounds. The optimized structures have been simulated in the commercial solver ESI-CEM [4]. The resulting input impedance data has been used in BetaMatch [2] to design matching networks for the structures. These networks, designed with real component models, have less than three components and yield better than -6.5dB matching in all considered bands.

The results presented in this paper suggest that the single frequency energy expressions (2.3), (2.4) and (2.5) may be useful for the design of antennas. The physical bounds described in [7, 9, 10] can be used to assess the feasibility of some designs.

Acknowledgment

The support of the Swedish Research Council is gratefully acknowledged.

References

[1] Antenna Standards Committee of the IEEE Antennas and Propagation Society. IEEE Standard Definitions of Terms for Antennas, 1993. IEEE Std 145-1993.

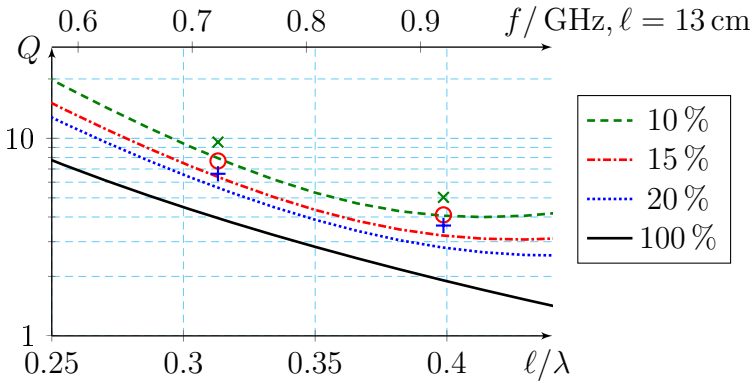

Figure 3: The Q factors (2.6) of the structures with antenna regions depicted in Fig. 2 middle column (top row "+," middle row "∘," and bottom row "×") compared with the physical bounds [7, 9] for rectangular structures with antenna regions 20%, 15%, and respectively 10% of the entire structure as in Fig. 1. The physical bound for structures limited to entire rectangular regions [8] is depicted in solid line (100%). The frequency scale for an $\ell = 13$ cm structure is included.

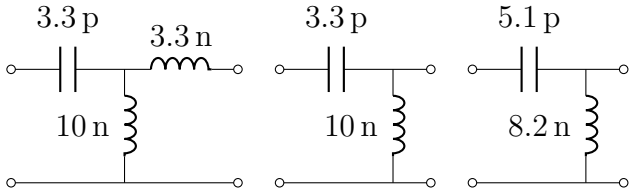

Figure 4: Matching networks for the structures with antenna regions depicted in Fig. 2 middle column, in SI units. From left to right the networks correspond to antenna regions extending 10%, 15% and respectively 20%.

[2] BetaMatch, Software for antenna component matching. http://www.mnw-scan.com/.

[3] M. Cismasu and M. Gustafsson. Antenna bandwidth optimization with single frequency simulation. *IEEE Trans. Antennas Propagat.*, 2014. (In press).

[4] ESI Group's computational electromagnetic (CEM) solution. http://www.esi-group.com.

[5] W. Geyi. A method for the evaluation of small antenna Q. *IEEE Trans. Antennas Propagat.*, **51**(8), 2124–2129, 2003.

[6] M. Gustafsson, M. Cismasu, and S. Nordebo. Absorption efficiency and physical bounds on antennas. *International Journal of Antennas and Propagation*, **2010**(Article ID 946746), 1–7, 2010.

[7] M. Gustafsson and S. Nordebo. Optimal antenna currents for Q, superdirectivity, and radiation patterns using convex optimization. *IEEE Trans. Antennas*

Propagat., **61**(3), 1109–1118, 2013.

[8] M. Gustafsson, C. Sohl, and G. Kristensson. Illustrations of new physical bounds on linearly polarized antennas. *IEEE Trans. Antennas Propagat.*, **57**(5), 1319–1327, May 2009.

[9] M. Gustafsson, M. Cismasu, and B. L. G. Jonsson. Physical bounds and optimal currents on antennas. *IEEE Trans. Antennas Propagat.*, **60**(6), 2672–2681, 2012.

[10] M. Gustafsson and B. Jonsson. Stored electromagnetic energy and antenna Q. Technical Report LUTEDX/(TEAT-7222)/1–25/(2012), Lund University, Department of Electrical and Information Technology, P.O. Box 118, S-221 00 Lund, Sweden, 2012. http://www.eit.lth.se.

[11] R. F. Harrington. *Field Computation by Moment Methods.* Macmillan, New York, 1968.

[12] J. M. Jin. *Theory and Computation of Electromagnetic Fields.* Wiley, 2011.

[13] J. M. Johnson and Y. Rahmat-Samii. Genetic algorithms and method of moments GA/MOM for the design of integrated antennas. *IEEE Trans. Antennas Propagat.*, **47**(10), 1606–1614, oct 1999.

[14] J. R. Mosig and F. E. Gardiol. A dynamical radiation model for microstrip structures. In P. W. Hawkes, editor, *Advances in Electronics and Electron Physics*, volume 59, pages 139 – 237. Academic Press, 1982.

[15] A. F. Peterson, S. L. Ray, and R. Mittra. *Computational Methods for Electromagnetics.* IEEE Press, New York, 1998.

[16] Y. Rahmat-Samii and E. Michielssen. *Electromagnetic Optimization by Genetic Algorithms.* Wiley Series in Microwave and Optical Engineering. John Wiley & Sons, 1999.

[17] B. Thors, H. Steyskal, and H. Holter. Broad-band fragmented aperture phased array element design using genetic algorithms. *IEEE Trans. Antennas Propagat.*, **53**(10), 3280 – 3287, oct. 2005.

[18] G. A. E. Vandenbosch. Reactive energies, impedance, and Q factor of radiating structures. *IEEE Trans. Antennas Propagat.*, **58**(4), 1112–1127, 2010.

[19] A. D. Yaghjian and S. R. Best. Impedance, bandwidth, and Q of antennas. *IEEE Trans. Antennas Propagat.*, **53**(4), 1298–1324, 2005.

Peter Johannesson, "Higher order hierarchical $H(\mathrm{curl})$ Legendre basis functions applied in the finite element method: emphasis on microwave circuits,"
LUTEDX/(TEAT-7205)/1-11/(2011).

Peter Johannesson and Anders Karlsson, "Numerical evaluation of potential integrals containing higher order hierarchical $H(\mathrm{div})$ Legendre basis functions for parameterized quadrilateral surface cells,"
LUTEDX/(TEAT-7206)/1-19/(2011).

Peter Johannesson, "Higher order hierarchical $H(\mathrm{curl})$ and $H(\mathrm{div})$ Legendre basis functions applied in hybrid FEM-MoM,"
LUTEDX/(TEAT-7207)/1-10/(2011).

Peter Johannesson and Anders Karlsson, "A quasi static iterative method for inductor parameter,"
LUTEDX/(TEAT-7208)/1-5/(2011).

Peter Johannesson, "On the evaluation of impedance matrix terms in MoM: emphasis on capacitive couplings,"
LUTEDX/(TEAT-7209)/1-9/(2011).

Mats Gustafsson, Marius Cismasu, and B.L.G. Jonsson, "Physical Bounds and Optimal Currents on Antennas,"
LUTEDX/(TEAT-7210)/1-22/(2011).

Sven Nordebo, Börje Nilsson, Thomas Biro, Gökhan Cinar, Mats Gustafsson, Stefan Gustafsson, Anders Karlsson, and Mats Sjöberg, "Electromagnetic dispersion modeling and measurements for HVDC power cables,"
LUTEDX/(TEAT-7211)/1-32/(2011).

Sven Nordebo, Börje Nilsson, Thomas Biro, Gökhan Cinar, Mats Gustafsson, Stefan Gustafsson, Anders Karlsson, and Mats Sjöberg, "Electromagnetic dispersion modeling and measurements for HVDC power cables,"
LUTEDX/(TEAT-7212)/1-20/(2011).

Mats Gustafsson, Iman Vakili, Sena E. Bayer, Daniel Sjöberg, Christer Larsson, "Optical theorem and forward scattering sum rule for periodic structures,"
LUTEDX/(TEAT-7213)/1-17/(2011).

Anders Bernland, "Bandwidth limitations for scattering of high order electromagnetic spherical waves with implications for the antenna scattering matrix,"
LUTEDX/(TEAT-7214)/1-22/(2011).

Anders Bernland, Mats Gustafsson, Carl Gustafson, and Fredrik Tufvesson, "Estimation of Spherical Wave Coefficients from 3D Positioner Channel Measurements,"
LUTEDX/(TEAT-7215)/1-11/(2012).

Mats Gustafsson and Sven Nordebo, "Antenna currents for optimal Q, superdirectivity, and radiation patterns using convex optimization,"
LUTEDX/(TEAT-7216)/1-21/(2012).

Mats Gustafsson, Jørgen Bach Andersen, Gerhard Kristensson, and Gert Frølund Pedersen, "Forward scattering of loaded and unloaded antennas,"
LUTEDX/(TEAT-7217)/1-13/(2012).

Anders Karlsson, Tan Yi, and Per-Erik Bengtsson, "Absorption and scattering of light from ensembles of randomly oriented aggregates,"
LUTEDX/(TEAT-7218)/1-20/(2012).

Jonas Fridén and Gerhard Kristensson, "Calculation of antenna radiation center using angular momentum,"
LUTEDX/(TEAT-7219)/1-21/(2012).

Gerhard Kristensson, "Electromagnetic scattering by a bounded obstacle in a parallel plate waveguide,"
LUTEDX/(TEAT-7220)/1-54/(2012).

Johan Helsing and Anders Karlsson, "An accurate boundary value problem solver applied to scattering from cylinders with corners,"
LUTEDX/(TEAT-7221)/1-16/(2012).

Mats Gustafsson and B. L. G. Jonsson, "Stored Electromagnetic Energy and Antenna Q,"
LUTEDX/(TEAT-7222)/1-25/(2012).

Kristin Persson, Mats Gustafsson, Gerhard Kristensson, and Björn Widenberg, "Radome diagnostics — source reconstruction of phase objects with an equivalent currents approach,"
LUTEDX/(TEAT-7223)/1-22/(2012).

Kristin Persson, Mats Gustafsson, Gerhard Kristensson, and Björn Widenberg, "Source reconstruction by far-field data for imaging of defects in frequency selective radomes,"
LUTEDX/(TEAT-7224)/1-14/(2013).

Michael Andersson, "Propagators and scattering of electromagnetic waves in planar bianisotropic slabs — an application to absorbers and frequency selective structures,"
LUTEDX/(TEAT-7225)/1-31/(2013).

Niklas Wellander and Gerhard Kristensson, "Estimates of scattered electromagnetic fields,"
LUTEDX/(TEAT-7226)/1-28/(2013).

Marius Cismasu and Mats Gustafsson, "Antenna Bandwidth Optimization with Single Frequency Simulation,"
LUTEDX/(TEAT-7227)/1-18/(2013).

Gerhard Kristensson, "Evaluation of an integral relevant to multiple scattering by randomly distributed obstacles,"
LUTEDX/(TEAT-7228)/1-13/(2014).

Iman Vakili, Mats Gustafsson, Daniel Sjöberg, Rebecca Seviour, Martin Nilsson, and Sven Nordebo, "Sum Rules for Parallel Plate Waveguides: Experimental Results and Theory,"
LUTEDX/(TEAT-7229)/1-20/(2014).

Marius Cismasu and Mats Gustafsson, "Multiband Antenna Q Optimization using Stored Energy Expressions,"
LUTEDX/(TEAT-7230)/1-9/(2014).